

1 **Supplement materials for**
2 **Kanaya et al., Long-term MAX-DOAS network observations of NO₂ in**
3 **Russia and Asia (MADRAS) during 2007–2012: instrumentation,**
4 **elucidation of climatology, and comparisons with OMI satellite**
5 **observations and global model simulations**
6

7 **Overview and Features of AOD**

8 The methodology used to derive AOD values at 476 nm is described in the main text, and the
9 results are briefly summarized in this supplementary material. A color index (defined as the
10 ratio of the intensities at 500 and 380 nm) was used to screen out cloudy cases. The threshold
11 values used for the color index are listed in Table S1. The threshold value for Cape Hedo was
12 changed from 1.50 (Takashima et al., 2009) to 2.40 (this study) with equivalence, because the
13 offsets at the two wavelengths were newly taken into account for the revised calculation of the
14 color index. For other locations, we tentatively determined the equivalent color index
15 threshold values based on the assumption that the color ratio under conditions where the sky
16 was the most whitish was similar to that at Cape Hedo; this provided calibration information
17 for the relative responses of the individual instruments at 380 and 500 nm.

18 Figure S1 shows the time series of monthly means of the AODs at six sites, with and
19 without cloud screening, based on the MAX-DOAS color index. The site-to-site differences
20 were not very large in comparison with those in the case of NO₂; in particular, the AOD levels
21 for Yokosuka (0.24 ± 0.05 (1σ)) as averages of monthly mean values after cloud screening, see
22 Table S2), an urban site, were similar to those at Cape Hedo (0.33 ± 0.13 (1σ)), a remote
23 island. Hefei had the highest average value (0.59 ± 0.13 (1σ)) among the studied locations.
24 The levels were roughly comparable to the climatological AOD values derived from satellite
25 sensors, i.e., Moderate Resolution Imaging Spectroradiometer (MODIS)/Terra, MODIS/Aqua,
26 and Multi-angle Imaging Spectroradiometer (MISR)/Terra (Fig. S1 and Table S2). The used
27 monthly average satellite data are from MODIS/Terra (Collection 5) and MODIS/Aqua
28 (Collection 5.1) at a $1^\circ \times 1^\circ$ grid resolution, and MISR/Terra (ver. 31) at a $0.5^\circ \times 0.5^\circ$ grid
29 resolution, available from the NASA Goddard Earth Sciences Data and Information Services
30 Center (<http://daac.gsfc.nasa.gov/giovanni/>). For the MODIS sensors, the AOD values at 550
31 nm were converted to those at 476 nm using the reported Ångström parameters. For MISR,
32 the Ångström parameters were estimated from the reported AOD values at multiple

33 wavelengths (443, 555, 670, and 865 nm), and then the AOD values at 476 nm were estimated.
34 Although the MODIS/Terra and MISR/Terra observations were made in the morning, and the
35 MODIS/Aqua observations were made in the afternoon, they were all compared with the
36 daytime averages of the MAX-DOAS observations. The AODs derived from MAX-DOAS
37 did not show significant diurnal variations (data not shown).

38 Similar seasonal variation patterns at remote islands (Cape Hedo and Fukue) were found
39 for the MAX-DOAS and satellite observations, with higher values in winter–spring as a result
40 of long-range transport from the Asian continent along the westerlies. The agreement was
41 excellent for Zvenigorod. Common increases in August 2010 were attributable to intense
42 forest/peat fires. At Yokosuka, the average MAX-DOAS AOD level with cloud screening was
43 more consistent with MISR than with MODIS (especially in summer), partly because of better
44 spatial resolution. Similar tendencies were found for Gwangju and Hefei. For Hefei, the
45 month-to-month variation patterns were qualitatively similar for MAX-DOAS and satellite
46 data. Comparisons with satellite data with finer spatial resolutions will be studied in the
47 future.

48 Figure S2 shows hourly-averaged AODs derived from MAX-DOAS and sky radiometer
49 (Aoki and Fujiyoshi, 2003) data at Fukue for 2009. The AOD value at 476 nm for sky
50 radiometer was calculated from the reported AOD value at 500 nm and the Ångström exponent.
51 A strong positive correlation was found around the 1:1 line. Similar comparisons with sky
52 radiometers and Mie lidar observations were successful at Tsukuba (Irie et al., 2008) and at
53 Cape Hedo (Takashima et al., 2009). Based on these features, we conclude that our AOD
54 products, with an estimated 30% uncertainty, are basically consistent with available
55 observations. As mentioned in the main text, 30% uncertainty in the AOD introduced only
56 10% or less uncertainty in the TropoNO₂VCD. Therefore the aerosol information can be
57 satisfactorily used to estimate NO₂ optimally and to study the general trends in the
58 OMI(NASA)/MAX-DOAS ratio of TropoNO₂VCD against the AOD.

59 **Table S1.** Recommended threshold values for color index used for cloud screening.

Instrument	Threshold value
Cape Hedo #1	2.40
Yokosuka #1	1.67
Fukue #1	0.81
Fukue #2	2.40
Fukue #3	1.55
Gwangju #1	2.20
Gwangju #2	2.10
Gwangju #3	2.02
Hefei #1	1.74
Hefei #2	2.01
Zvenigorod #1	1.57

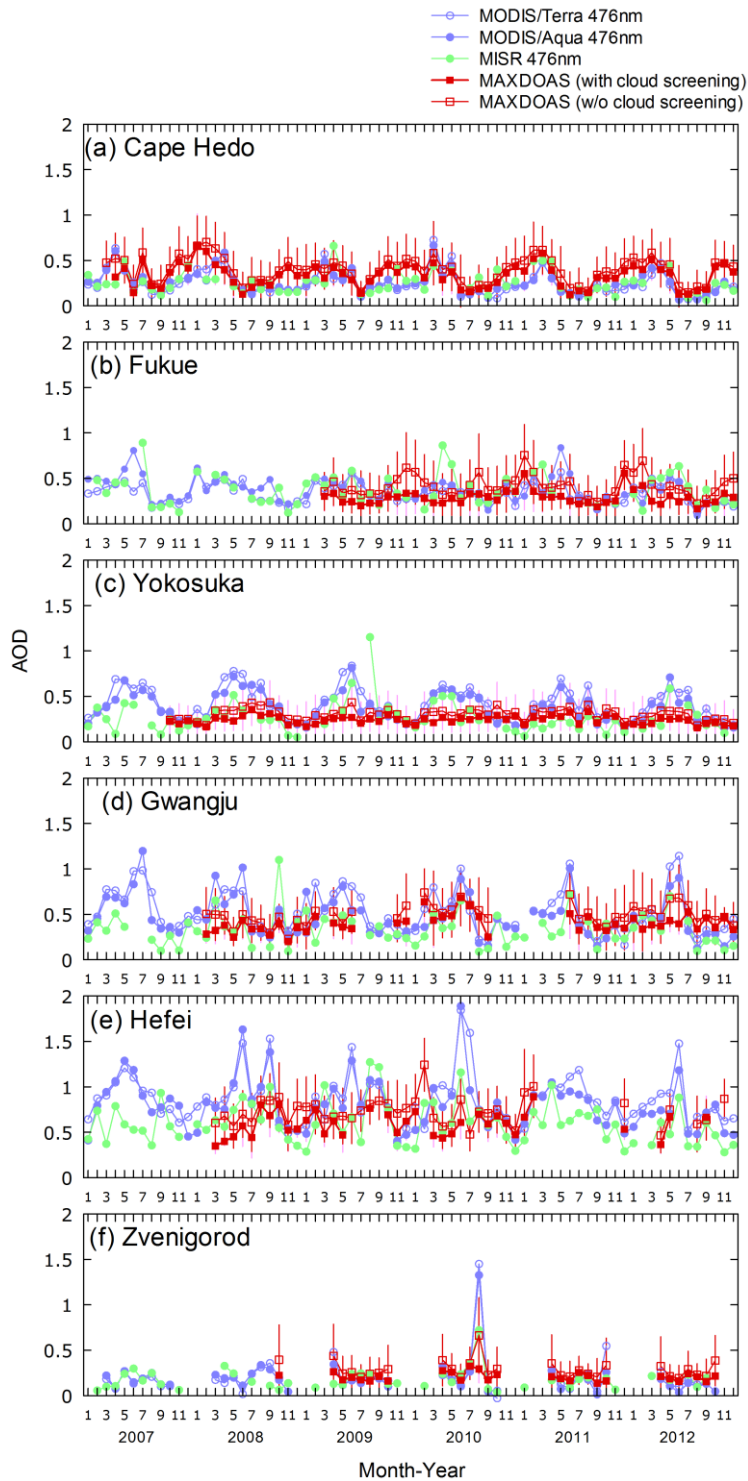
60

61 **Table S2.** Averages and 1σ ranges of monthly mean AOD values derived from MAX-DOAS

62 observations and satellite observations.

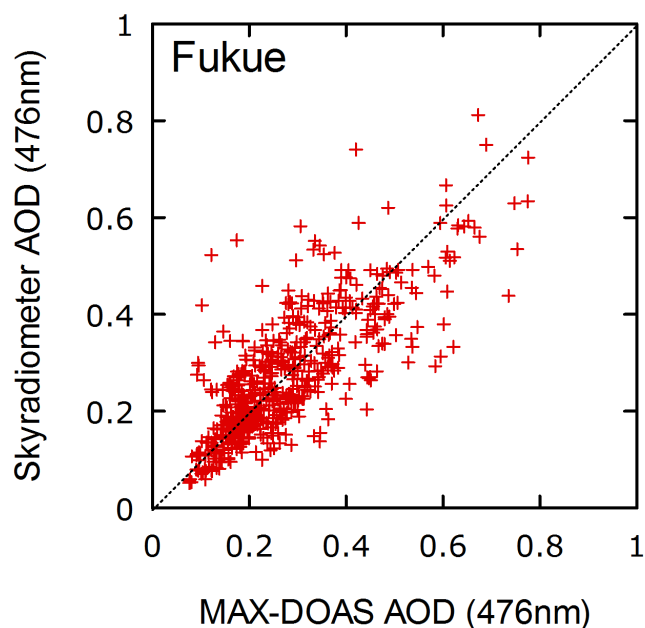
	MAX-DOAS (with cloud screening)	MAX-DOAS (without cloud screening)	MODIS/Terra	MODIS/Aqua	MISR/Terra
Cape Hedo	0.33 ± 0.13	0.40 ± 0.14	0.26 ± 0.13	0.25 ± 0.14	0.26 ± 0.12
Yokosuka	0.24 ± 0.05	0.30 ± 0.06	0.37 ± 0.16	0.42 ± 0.18	0.27 ± 0.17
Fukue	0.29 ± 0.08	0.42 ± 0.12	0.38 ± 0.14	0.34 ± 0.12	0.37 ± 0.17
Gwangju	0.40 ± 0.10	0.50 ± 0.11	0.47 ± 0.23	0.53 ± 0.23	0.33 ± 0.18
Hefei	0.59 ± 0.13	0.73 ± 0.15	0.80 ± 0.28	0.86 ± 0.28	0.60 ± 0.23
Zvenigorod	0.21 ± 0.05	0.29 ± 0.10	0.19 ± 0.19	0.21 ± 0.22	0.18 ± 0.11

63



64

65 **Fig. S1.** Time series of monthly averages of AOD derived from MAX-DOAS and satellite
 66 observations. The satellite observations are derived using MODIS and MISR sensors on board
 67 Terra and Aqua. MAX-DOAS data, with and without cloud screening, are provided with error
 68 bars representing the 1σ range of the included data.



69
 70 **Fig. S2.** Scatterplot between AODs observed by MAX-DOAS and a sky radiometer at Fukue
 71 site in 2009.

72

73

74 **References**

75 Aoki, K, and Fujiyoshi, Y.: Sky radiometer measurements of aerosol optical properties over
 76 Sapporo, Japan. *J. Meteorol Soc. Jpn.*, 81, 493-513, 2003.

77 Irie, H., Kanaya, Y., Akimoto, H., Iwabuchi, H., Shimizu, A., and Aoki, K.: First retrieval of
 78 tropospheric aerosol profiles using MAX-DOAS and comparison with lidar and sky
 79 radiometer measurements, *Atmos. Chem. Phys.*, 8, 341-350, 2008.

80 Takashima, H., Irie, H., Kanaya, Y., Shimizu, A., Aoki, K., and Akimoto, H.: Atmospheric
 81 aerosol variations at Okinawa Island in Japan observed by MAX-DOAS using a new
 82 cloud-screening method, *J. Geophys. Res.*, 114, D18213, doi:10.1029/2009JD011939,
 83 2009.

84

85